

Pt^{II} and Pt^{III} dimers containing a Pt₂(2,2'-bipyridine)₂(μ-*N,N*-dimethylguanidinato)₂ unit

 Ken Sakai,^{a*} Kazuo Yokokawa^b and Yoshimi Yokoyama^a

^aDepartment of Chemistry, Faculty of Science, Kyushu University, Hakozaki 6-10-1, Higashi-ku, Fukuoka 812-8581, Japan, and ^bDepartment of Applied Chemistry, Faculty of Science, Science University of Tokyo, Kagurazaka 1-3, Shinjuku-ku, Tokyo 162-8601, Japan

Correspondence e-mail: ksakaiscc@mbox.nc.kyushu-u.ac.jp

Received 15 November 2006

Accepted 11 December 2006

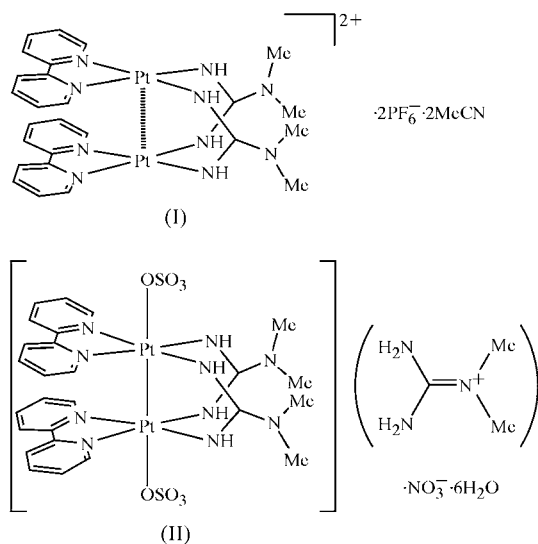
Online 13 January 2007

The syntheses and crystal structures of the title Pt^{II} and Pt^{III} dimers doubly bridged with *N,N*-dimethylguanidinate ligands, namely bis(μ-*N,N*-dimethylguanidinato)bis[(2,2'-bipyridine)-platinum(II)](*Pt*–*Pt*) bis(hexafluorophosphate) acetonitrile disolvate, [Pt^{II}₂(C₃H₈N₃)₂(C₁₀H₈N₂)₂](PF₆)₂·2CH₃CN, (I), and guanidinium bis(μ-*N,N*-dimethylguanidinato)bis[(2,2'-bipyridine)sulfatoplatinum(III)](*Pt*–*Pt*) bis(hexafluorophosphate) nitrate hexahydrate, (C₃H₁₀N₃)[Pt^{III}₂(C₃H₈N₃)₂(SO₄)₂(C₁₀H₈N₂)₂][NO₃·6H₂O], (II), are reported. The oxidation of the Pt^{II} dimer into the Pt^{III} dimer results in a marked shortening of the Pt–Pt distance from 2.8512 (6) to 2.5656 (4) Å. The change is mainly compensated for by the change in the dihedral angle between the two Pt coordination planes upon oxidation, from 21.9 (2) to 16.9 (3)°. We attribute the relatively strong one-dimensional stack of dimers achieved in the Pt^{II} compound in part to the strong Pt^{II}···C(bpy) associations (bpy is 2,2'-bipyridine) in the crystal structure [Pt···C = 3.416 (10) and 3.361 (12) Å].

Comment

One-dimensional materials have attracted considerable attention due to their highly anisotropic physical properties. In order to develop new types of one-dimensional substances, interest has for many years concentrated on the use of dinuclear entities as the repeating units, since the electronic structures at the metal centres may be controlled prior to the formation of a one-dimensional stack of dimers. In this context, we reported previously that *cis*-diammineplatinum dimers doubly bridged with carboxylate ligands afford a new series of one-dimensional platinum chain compounds with the general formula [Pt₂(NH₃)₄(μ-carboxylato)₂]_n^{m+}, where the charge *m* depends on the average Pt oxidation state (Sakai, Takeshita *et al.*, 1998; Sakai *et al.*, 2002). One of the attractive features of these dimeric units is that they are doubly bridged by carboxylate ligands in a *cis* fashion, leading to high flex-

ibility in their Pt–Pt distances upon formation of this bond as the partial oxidation at the metal centres proceeds (Sakai, Tanaka *et al.*, 1998). As an extension of studies of such



carboxylate systems, we have also developed a new one-dimensional platinum family by combining a cationic diplatinum complex with an anionic mononuclear complex, *e.g.* [Pt^{II}₂(bpy)₂(μ-pivalamidato)₂]²⁺ and [Pt^{II}(oxalato)₂]²⁻ (bpy is 2,2'-bipyridine; Akiyama *et al.*, 2000). In that study, a very intriguing alternating stack of dimers and monomers was found in the crystal structure. It was also found that the so-called 'HT–HH' isomerization of the pivalamidate-bridged dimer took place to give a mixture of two isomers, where HT and HH correspond to the head-to-tail and head-to-head arrangements, respectively, of the bridging amidate ligands. The co-existence of these two isomers caused difficulties in evaluating the crystal structures and their oligomerization behaviours in aqueous media. For instance, even if a pure HT dimer, *e.g.* HT-[Pt^{II}₂(bpy)₂(μ-pivalamidato)₂](NO₃)₂·5H₂O, is employed as the starting material, in aqueous media the dimer gradually undergoes HT–HH isomerization over a day to give a mixture of two isomers (Sakai, 1996). In order to avoid such complications, dimers bridged by guanidinate derivatives,

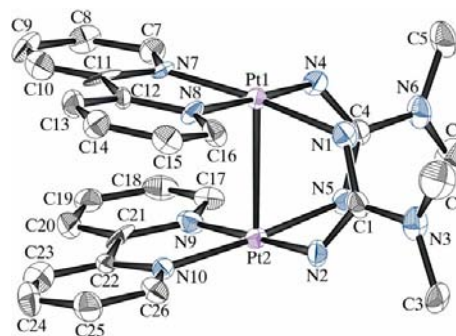
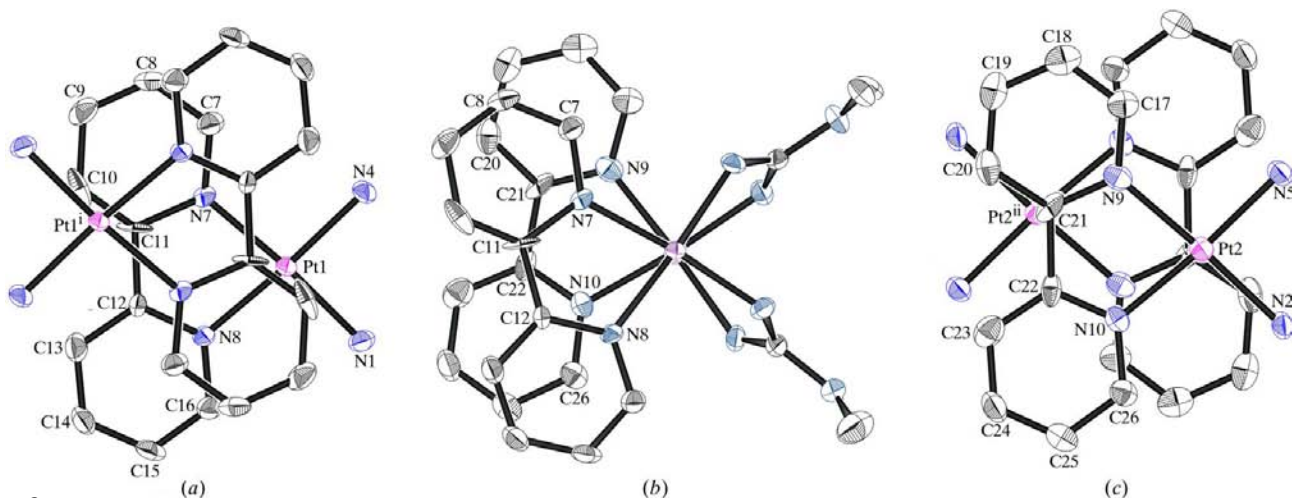
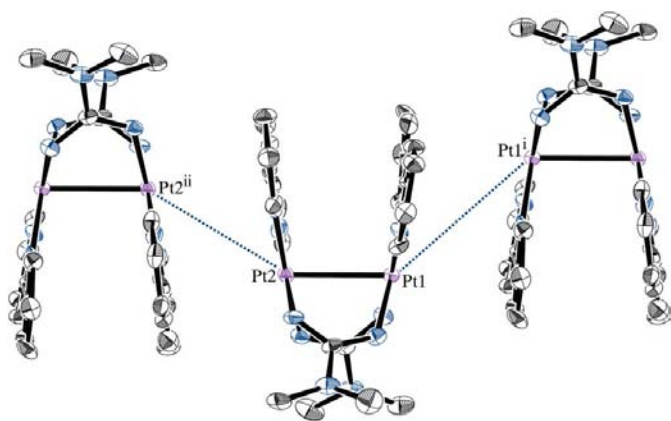


Figure 1
The structure of (I), showing the atom-labelling scheme. Displacement ellipsoids are drawn at the 50% probability level. H atoms have been omitted for clarity.

**Figure 2**

Views showing three different stacking interactions within the one-dimensional column in (I). (a) The interdimer association of the $\text{Pt1} \cdots \text{Pt1}^i$ geometry. (b) The intradimer association (labels are only given for the atoms used to estimate the intradimer bpy-to-bpy separation). (c) The interdimer association of the $\text{Pt2} \cdots \text{Pt2}^{ii}$ geometry. H atoms have been omitted for clarity. [Symmetry codes: (i) $-x, -y, 1-z$; (ii) $-x, -y, -z$.]

**Figure 3**

A side view, showing the way in which three adjacent dimer cations stack to give a one-dimensional chain in (I). Each dimer-dimer interaction is correlated with an inversion centre. H atoms have been omitted for clarity. [Symmetry codes: (i) $-x, -y, 1-z$; (ii) $-x, -y, -z$.]

e.g. $[\text{Pt}_2^{\text{II}}(\text{bpy})_2(\mu\text{-bridge})_2]^{2+}$ (bridge is guanidinate, *N,N*-dimethylguanidinate, *N,N*-diethylguanidinate, etc.), have been examined in our recent studies, since these dimers afford only one isomer (bridging amidates coordinate with N- and O-atom donors, while bridging guanidates coordinate with two chemically equivalent N-atom donors). We report here the syntheses and crystal structures of the Pt_2^{II} and Pt_2^{III} dimers bridged by *N,N*-dimethylguanidinate (dmg) ligands, viz. $[\text{Pt}_2^{\text{II}}(\text{bpy})_2(\mu\text{-dmg})_2](\text{PF}_6)_2 \cdot 2\text{CH}_3\text{CN}$, (I), and $[\text{Pt}_2^{\text{III}}(\text{bpy})_2(\text{SO}_4)_2(\mu\text{-dmg})_2](\text{dmgH}_2)(\text{NO}_3) \cdot 6\text{H}_2\text{O}$, (II).

The asymmetric unit of (I) consists of a dinuclear platinum(II) cation (Fig. 1), two PF_6^- anions and two acetonitrile solvent molecules. The two square-planar Pt^{II} coordination planes are doubly bridged by the *N,N*-dimethylguanidinate ligands in a *cis* fashion. The dihedral angle between the two coordination planes (τ) is $21.9(2)^\circ$, where each coordination

plane is defined by four coordinated N atoms. In the mean-plane calculations, the r.m.s. deviations are $0.033(9) \text{ \AA}$ for N1/N4/N7/N8 and $0.013(3) \text{ \AA}$ for N2/N5/N9/N10. The average torsional twist of these coordination planes about the $\text{Pt} \cdots \text{Pt}$ vector (ω) is $22.5(10)^\circ$. Atoms Pt1 and Pt2 are displaced out of their respective least-squares mean planes by $0.038(5)$ and $0.036(5) \text{ \AA}$, suggesting that they have a mutually repulsive interaction. Alternatively, it may be considered that the two N(bpy) atoms in each Pt coordination plane are shifted out of the coordination plane due to the attractive $\pi\text{-}\pi$ interaction within the dimeric unit. Very similar structural features were previously observed for $[\text{Pt}_2^{\text{II}}(\text{phen})_2(\mu\text{-pivalamidato})_2](\text{NO}_3)_2 \cdot 2\text{H}_2\text{O}$ (phen is 1,10-phenanthroline) [hereinafter (III); $\tau = 21.5(4)^\circ$ and $\omega = 13(3)^\circ$; Sakai *et al.*, 2003]. The two pyridyl rings attached to atom Pt1 are twisted about the central C11–C12 bond: $\text{N7}-\text{C11}-\text{C12}-\text{N8} = -5.4(13)^\circ$ and $\text{C10}-\text{C11}-\text{C12}-\text{C13} = -3.4(19)^\circ$. These two pyridyl planes are canted at an angle of $5.4(3)^\circ$. In contrast, the bpy ligand bound to atom Pt2 possesses a planar geometry, with a 12-atom r.m.s. deviation of $0.02(2) \text{ \AA}$.

The two bpy ligands within the dimeric unit form a π -stacking interaction. The intradimer bpy-to-bpy separation, defined as the separation between the N7/N8/C7/C8/C11/C12 and N9/N10/C20/C21/C22/C26 planes, is $3.45(15) \text{ \AA}$ (Fig. 2b). The intradimer $\text{Pt} \cdots \text{Pt}$ distance [$2.8512(6) \text{ \AA}$] is comparable with the value of $2.8489(17) \text{ \AA}$ reported for (III). The interdimer $\text{Pt} \cdots \text{Pt}$ distances [$\text{Pt1}^i \cdots \text{Pt1}^i = 4.9369(9) \text{ \AA}$ and $\text{Pt2} \cdots \text{Pt2}^{ii} = 4.5660(9) \text{ \AA}$; symmetry codes: (i) $-x, -y, 1-z$; (ii) $-x, -y, -z$] reveal that there is no significant intermolecular metal-metal interaction in the crystal structure (Fig. 3). Nevertheless, as previously observed for (III), the dimer units stack along the *c* axis in a one-dimensional fashion based on relatively strong $\pi(\text{bpy})\text{-}\pi(\text{bpy})$ and $d(\text{Pt})\text{-}\pi(\text{bpy})$ interactions [$\text{Pt1} \cdots \text{C11}^i = 3.416(10) \text{ \AA}$, $\text{Pt1} \cdots \text{C10}^i = 3.470(13) \text{ \AA}$ and $\text{Pt2} \cdots \text{C21}^{ii} = 3.361(12) \text{ \AA}$], which is obviously relevant to the dark-red colour of the material (see also Figs. 2a, 2c and 4).

metal-organic compounds

The interplanar separation for the $\text{Pt1} \cdots \text{Pt1}(-x, -y, 1 - z)$ stack is 3.31 (4) Å, while the corresponding value for $\text{Pt2} \cdots \text{Pt2}(-x, -y, -z)$ is 3.34 (1) Å. These values refer to the stacking of two crystallographically equivalent planes, related by an inversion centre in each case, the planes being Pt1/N7/N8/C7/C8/C10/C11/C12 and Pt2/N9/N10/C17/C18/C21/C22/C26, respectively.

The asymmetric unit of (II) consists of a neutral Pt_2^{III} dimer (Fig. 5), a guanidinium cation, a nitrate anion, and six solvent water molecules. The axial sites of the dinuclear platinum(III) unit are occupied by sulfate O atoms. An interesting structural feature is that each sulfate anion is doubly hydrogen bonded to the N–H(dmg) groups (Table 4). The non-coordinated guanidinium cation is also hydrogen bonded to one of the coordinated sulfate anions [$\text{N11} \cdots \text{O4} = 2.973$ (11) Å and $\text{N12} \cdots \text{O2} = 2.962$ (10) Å; Table 4]. The bridged Pt \cdots Pt distance [2.5656 (4) Å] is very close to the value of 2.5664 (6) Å reported for the pivalamidate-bridged analogue [$\text{Pt}_2^{\text{III}}(\text{bpy})_2(\mu\text{-pivalamidato})_2(\text{SO}_4)_2 \cdot 4\text{H}_2\text{O}$ hereinafter (IV); Yokokawa & Sakai, 2004]. This is the second example of a crystal structure of a platinum(III) dimer with the general formula $[\text{Pt}_2^{\text{III}}(\text{bpy})_2(\mu\text{-bridge})_2L_2]$ (bridge is amidate, carboxylate, guanidinate, *etc.*; L is an axial ligand such as OH_2 ,

Cl^- , SO_4^{2-} or NO_3^-). The $\text{Pt}^{\text{III}}\text{—O}(\text{sulfate})$ distances [2.152 (5) and 2.139 (5) Å] are also similar to the value of 2.144 (7) Å reported for (IV). In this paper, an equatorial coordination plane within an overall octahedral geometry is defined for each Pt^{III} ion as the plane which is perpendicular to the $\text{Pt}^{\text{III}} \cdots \text{Pt}^{\text{III}}$ axis. Thus, one equatorial Pt^{III} coordination plane is defined by N1/N4/N7/N8 and the other by N2/N5/N9/N10, with a dihedral angle between them of 16.9 (3)° and a mean torsional twist of 18 (1)°. These indicate that the shortening of *ca* 0.29 Å in the Pt \cdots Pt distance upon oxidation of (I) to (II) is mainly compensated for by the change in τ , giving only a small change in ω . The mean-plane calculations performed for the four-coordinated equatorial donor atoms

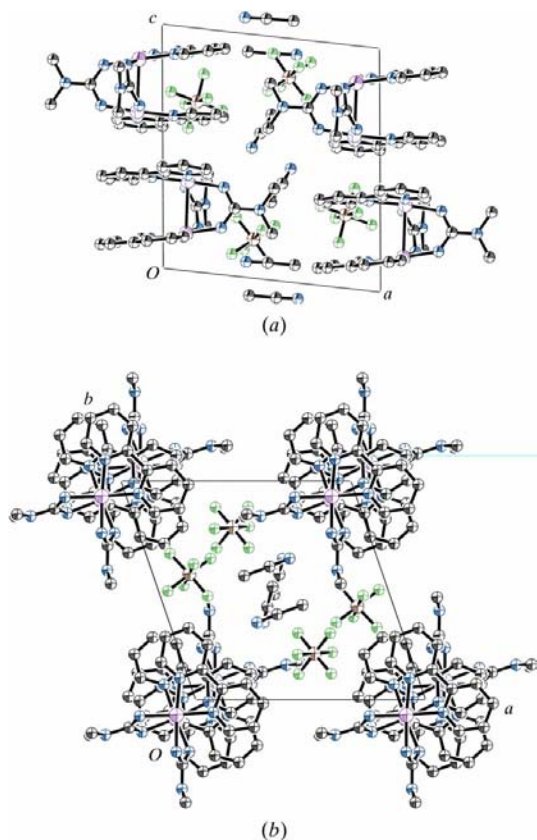


Figure 4
Crystal packing views, showing one-dimensional columns consisting of dimer units (a) along the b axis and (b) along the c axis. For clarity, only one of the two disordered sites (site A) is plotted for each PF_6^- anion. H atoms have been omitted for clarity.

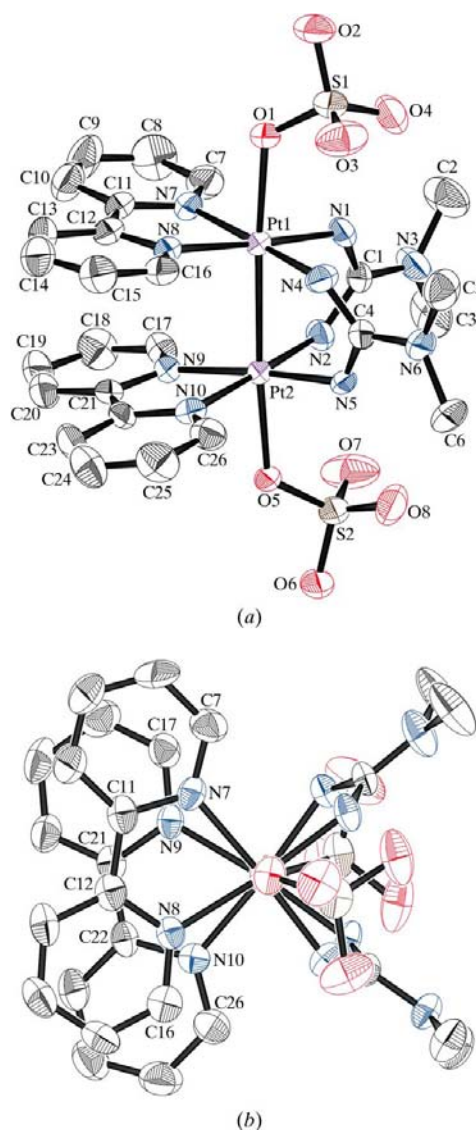


Figure 5
Views of (II), showing (a) a side view and (b) a top view down the $\text{Pt1} \cdots \text{Pt2}$ vector, together with the atom-labelling scheme. For (b), only those atoms involved in significant intramolecular $\pi\text{—}\pi$ associations are labelled. Displacement ellipsoids are drawn at the 50% probability level. H atoms have been omitted for clarity.

reveal both planes to be planar, with r.m.s. deviations of 0.0004 (2) Å for N1/N4/N7/N8 and 0.007 (2) Å for N2/N5/N9/N10. Atoms Pt1 and Pt2 are displaced towards each other out of the local equatorial coordination plane by 0.016 (3) and 0.027 (3) Å, respectively.

As shown in Fig. 5(b) and Table 3, the two bpy planes show short stacking interactions due to the formation of a Pt^{III}–Pt^{III} single bond. The net separation between the stacked bpy moieties is estimated as 3.2 (2) Å, which is calculated from the separation between the C7/N7/C11/C12/N8/C16 and C17/N9/C21/C22/N10/C26 planes. Such short C···C contacts have previously been observed for some special cases [see, for example, the value of the C···C separation [3.252 (2) Å] reported for a one-dimensional-stacked nickel phthalocyanine complex (Schramm *et al.*, 1980)]. The two bpy planes defined by N7/N8/C7–C16 and N9/N10/C17–C26 exhibit r.m.s. deviations of 0.03 (3) and 0.04 (3) Å, respectively. Moreover, each bpy plane is nearly coplanar with the local equatorial coor-

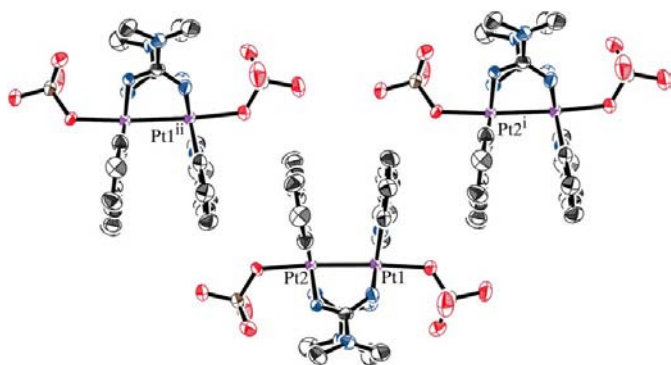


Figure 6
A side view of (II), showing three adjacent dimer units stacked in the [101] direction. H atoms have been omitted for clarity. [Symmetry codes: (i) $\frac{1}{2} + x, \frac{1}{2} - y, \frac{1}{2} + z$; (ii) $-\frac{1}{2} + x, \frac{1}{2} - y, -\frac{1}{2} + z$.]

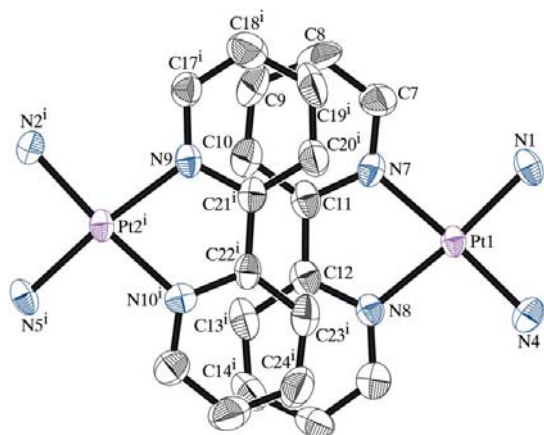


Figure 7
A view showing the stacking of adjacent dimer units in (II). H atoms have been omitted for clarity. [Symmetry code: (i) $\frac{1}{2} + x, \frac{1}{2} - y, \frac{1}{2} + z$.]

dination plane: the dihedral angle between the N1/N4/N7/N8 and N7/N8/C7–C16 planes is 1.6 (3)°, while the corresponding angle between the N2/N5/N9/N10 and N9/N10/C17–C26 planes is 0.4 (3)°.

The dimer further forms a one-dimensional stack in the [101] direction *via* π – π stacking interactions between adjacent dimers (Fig. 6). However, the separation between adjacent bpy planes is estimated as 3.68 (4) Å (see also Fig. 7), indicating that the intermolecular π – π associations in (II) are relatively weak in comparison with those achieved in (I). This implies that the $d(\text{Pt}^{\text{II}})$ – $\pi(\text{bpy})$ interactions achieved in (I) contribute significantly to the relatively strong interdimer stacking associations in (I).

Experimental

In order to avoid complexation between the silver ion and the *N,N*-dimethylguanidinate ligand, compounds (I) and (II) were prepared from a hydroxo-bridged dimer, $[\text{Pt}_2(\mu\text{-OH})_2(\text{bpy})_2](\text{NO}_3)_2$ (Wimmer *et al.*, 1988). It is also noteworthy that the preparation of the pivalamide-bridged analogue was carried out as a one-pot reaction of $\text{PtCl}_2(\text{bpy})$, silver nitrate and pivalamide (Yokokawa & Sakai, 2004).

For the synthesis of (I), a solution of $\text{PtCl}_2(\text{bpy})$ (0.5 mmol, 0.221 g) and AgNO_3 (1.0 mmol, 0.170 g) in water (10 ml) was refluxed in the dark for 3 h, followed by filtration to remove the precipitated AgCl . To the filtrate were added $[(\text{CH}_3)_2\text{NC}(\text{NH})\text{NH}_2]\cdot\text{H}_2\text{SO}_4$ (0.375 mmol, 0.102 g) and methanol (10 ml). After adjusting the pH of the mixture to 8, the solution was refluxed for 24 h, during which time the colour of the solution turned red–purple. The solution was then left at room temperature, followed by filtration to remove insoluble material. To the resulting filtrate were added 7–8 drops of a saturated aqueous NH_4PF_6 solution. The resulting deep-green powder was collected by filtration and dried *in vacuo* (yield 0.11 g). The crude product was purified on a Sephadex LH-20 column using MeOH – CH_3CN (1:1 *v/v*) as eluent. The first and second deep-brown bands were assumed to correspond to compounds of higher nuclearity, although their identification has been unsuccessful so far. The third red–purple band, corresponding to (I), was collected and the solution evaporated to dryness. The compound was redissolved in CH_3CN and recrystallized by leaving the solution at room temperature in air in a vial covered with aluminium foil, with several pin holes made in the foil to allow the slow evaporation of the solvent (yield 9.6%). The acetonitrile solvate, (I), easily loses solvent upon exposure to air, so single-crystal X-ray diffractometry was carried out on the solvated form. All other analytical data were obtained for the non-solvated form of the complex, $[\text{Pt}_2^{\text{II}}(\text{bpy})_2(\mu\text{-dmg})_2](\text{PF}_6)_2$, as follows: analysis calculated for $\text{C}_{26}\text{H}_{32}\text{F}_{12}\text{N}_{10}\text{P}_2\text{Pt}_2$: C 26.81, H 2.77, N 12.03%; found: C 26.54, H 2.48, N 11.44%. IR (KBr, ν , cm^{-1}): 3419 (*w*), 1607 (*w*), 1547 (*m*), 1453 (*w*), 1318 (*w*), 1176 (*w*), 1065 (*w*), 840 (*s*), 768 (*w*), 558 (*m*); ^1H NMR (CD_3CN): δ 3.08 (*s*, 12H, methyl), 3.61 (*s*, 4H, NH), 7.35 (*t*, 4H, bpy), 7.54 (*d*, 4H, bpy), 8.02 (*t*, 4H, bpy), 8.70 (*d*, 4H, bpy); UV–vis absorption spectrum (CH_3CN , 293 K, in air): 500 ($\epsilon = 1990 \text{ M}^{-1} \text{ cm}^{-1}$, metal–metal-to-ligand charge-transfer band), 312 nm ($\epsilon = 18100 \text{ M}^{-1} \text{ cm}^{-1}$) and 251 nm ($\epsilon = 37800 \text{ M}^{-1} \text{ cm}^{-1}$).

For the synthesis of (II), a solution of $\text{PtCl}_2(\text{bpy})$ (0.5 mmol, 0.221 g) and AgNO_3 (1.0 mmol, 0.170 g) in water (10 ml) was refluxed in the dark for 3 h, followed by filtration to remove the precipitated AgCl . The filtrate was then evaporated to dryness to give a solid

corresponding to [Pt₂(μ-OH)₂(bpy)₂](NO₃)₂ (Wimmer *et al.*, 1988). To this were added [(CH₃)₂NC(:NH)NH₂]₂·H₂SO₄ (0.375 mmol, 0.102 g) and water (2.5 ml). The solution was refluxed for 24 h, during which time the colour of the solution changed to red. The solution was allowed to stand at room temperature in air for a few days until the volume of the solution was greatly reduced. The deposited product consisted of red crystals of an unidentified by-product and orange prisms of (II). These two types of crystals were collected by filtration, dried in air and manually separated under a microscope. The total yield of the orange compound, (II), was 87 mg (13%). Analysis calculated for C₂₉H₅₄N₁₄O₁₇Pt₂S₂: C 26.29, H 4.11, N 14.80%; found: C 26.43, H 3.34, N 15.10%. IR (KBr, ν, cm⁻¹): 3364 (*m, br*), 1636 (*m*), 1603 (*m*), 1573 (*m*), 1541 (*m*), 1384 (*s*), 1118 (*s*), 1030 (*w*), 766 (*m*), 618 (*s*), 420 (*w*).

Compound (I)

Crystal data

[Pt₂(C₃H₈N₃)₂(C₁₀H₈N₂)₂](PF₆)₂·2C₂H₅N
M_r = 1246.84
 Triclinic, P1̄
a = 12.527 (1) Å
b = 12.606 (1) Å
c = 13.3233 (11) Å
 α = 94.945 (1)°
 β = 94.621 (1)°
 γ = 108.295 (1)°
V = 1977.3 (3) Å³
Z = 2
D_x = 2.094 Mg m⁻³
 Mo Kα radiation
 μ = 7.25 mm⁻¹
T = 100 (1) K
 Square prism, dark red
 0.21 × 0.16 × 0.09 mm

Data collection

Bruker SMART APEX CCD area-detector diffractometer
 ω scans
 Absorption correction: multi-scan (SADABS; Sheldrick, 1996)
T_{min} = 0.384, *T_{max}* = 0.521
 23482 measured reflections
 8671 independent reflections
 6882 reflections with *I* > 2σ(*I*)
R_{int} = 0.045
θ_{max} = 27.1°

Refinement

Refinement on *F*²
R[*F*² > 2σ(*F*²)] = 0.061
wR(*F*²) = 0.154
S = 1.15
 8671 reflections
 497 parameters
 H-atom parameters constrained
w = 1/[σ²(*F_o*²) + (0.0584*P*)² + 40.2739*P*]
 where *P* = (*F_o*² + 2*F_c*²)/3
 (Δσ)_{max} < 0.001
 Δρ_{max} = 4.41 e Å⁻³
 Δρ_{min} = -2.80 e Å⁻³

Table 1

Selected geometric parameters (Å, °) for (I).

Pt1—Pt2	2.8512 (6)	Pt2—N2	2.030 (10)
Pt1—N1	1.993 (10)	Pt2—N5	2.005 (10)
Pt1—N4	2.016 (9)	Pt2—N9	2.027 (11)
Pt1—N7	2.016 (9)	Pt2—N10	2.014 (9)
Pt1—N8	2.019 (9)		
Pt1...C11 ⁱ	3.416 (10)	Pt2...C21 ⁱⁱ	3.361 (12)
Pt1...C10 ⁱ	3.470 (13)		
N1—Pt1—N4	88.3 (4)	N5—Pt2—N10	174.7 (4)
N1—Pt1—N7	174.1 (4)	N5—Pt2—N9	95.1 (4)
N4—Pt1—N7	96.0 (4)	N10—Pt2—N9	80.4 (4)
N1—Pt1—N8	95.3 (4)	N5—Pt2—N2	87.6 (4)
N4—Pt1—N8	176.4 (4)	N10—Pt2—N2	96.9 (4)
N7—Pt1—N8	80.4 (4)	N9—Pt2—N2	177.0 (4)
N4—Pt1—Pt2—N5	22.0 (4)	N7—Pt1—Pt2—N9	23.4 (4)
N8—Pt1—Pt2—N10	23.2 (4)	N1—Pt1—Pt2—N2	21.3 (4)

Symmetry codes: (i) -*x*, -*y*, -*z* + 1; (ii) -*x*, -*y*, -*z*.

Table 2

Selected geometric parameters (Å, °) for (II).

Pt1—Pt2	2.5656 (4)	Pt2—N5	1.988 (6)
Pt1—N1	1.994 (6)	Pt2—N9	2.045 (6)
Pt1—N4	1.980 (6)	Pt2—N10	2.032 (6)
Pt1—N7	2.060 (6)	Pt1—O1	2.152 (5)
Pt1—N8	2.041 (6)	Pt2—O5	2.139 (5)
Pt2—N2	1.992 (6)	Pt1—Pt2 ⁱ	7.5991 (4)
N7...N9	3.157 (8)	N10...C16	3.244 (10)
N7...C17	3.263 (10)	C7...C17	3.324 (12)
N8...N10	3.135 (8)	C12...C21	3.429 (10)
N8...C22	3.382 (9)	C16...C26	3.278 (11)
N9...C11	3.352 (9)		
N4—Pt1—N1	89.2 (3)	N5—Pt2—N2	90.4 (3)
N4—Pt1—N8	96.0 (3)	N5—Pt2—N10	94.5 (3)
N1—Pt1—N8	174.7 (3)	N2—Pt2—N10	175.0 (3)
N4—Pt1—N7	176.4 (3)	N5—Pt2—N9	173.7 (3)
N1—Pt1—N7	94.3 (3)	N2—Pt2—N9	95.6 (3)
N8—Pt1—N7	80.5 (3)	N10—Pt2—N9	79.6 (3)
N4—Pt1—O1	93.7 (2)	N5—Pt2—O5	92.0 (2)
N1—Pt1—O1	92.0 (2)	N2—Pt2—O5	93.6 (2)
N8—Pt1—O1	86.7 (2)	N10—Pt2—O5	85.0 (2)
N7—Pt1—O1	85.3 (2)	N9—Pt2—O5	85.7 (2)
N4—Pt1—Pt2—N5	-16.3 (3)	N8—Pt1—Pt2—N10	-17.9 (3)
N1—Pt1—Pt2—N2	-17.5 (3)	N7—Pt1—Pt2—N9	-18.6 (3)

Symmetry code: (i) *x* + ½, -*y* + ½, *z* + ½.

Compound (II)

Crystal data

(C₃H₁₀N₃)[Pt₂(C₃H₈N₃)₂(SO₄)₂·(C₁₀H₈N₂)₂]NO₃·6H₂O
M_r = 1325.16
 Monoclinic, *P*2₁/*n*
a = 12.6189 (6) Å
b = 28.9553 (14) Å
c = 14.4197 (7) Å
 β = 114.712 (1)°
V = 4786.2 (4) Å³
Z = 4
D_x = 1.839 Mg m⁻³
 Mo Kα radiation
 μ = 6.01 mm⁻¹
T = 296 (2) K
 Square prism, orange
 0.25 × 0.14 × 0.07 mm

Data collection

Bruker SMART APEX CCD area-detector diffractometer
 ω scans
 Absorption correction: Gaussian (XPREP in SAINTE; Bruker, 2001)
T_{min} = 0.272, *T_{max}* = 0.676
 31986 measured reflections
 11376 independent reflections
 6677 reflections with *I* > 2σ(*I*)
R_{int} = 0.066
θ_{max} = 27.9°

Refinement

Refinement on *F*²
R[*F*² > 2σ(*F*²)] = 0.041
wR(*F*²) = 0.114
S = 0.95
 11376 reflections
 568 parameters
 H-atom parameters constrained
w = 1/[σ²(*F_o*²) + (0.0459*P*)²]
 where *P* = (*F_o*² + 2*F_c*²)/3
 (Δσ)_{max} = 0.003
 Δρ_{max} = 2.15 e Å⁻³
 Δρ_{min} = -1.07 e Å⁻³

Table 3

Contact distances for (II) (Å).

N7...N9	3.157 (8)	N10...C16	3.244 (10)
N7...C17	3.263 (10)	C7...C17	3.324 (12)
N8...N10	3.135 (8)	C12...C21	3.429 (10)
N8...C22	3.382 (9)	C16...C26	3.278 (11)
N9...C11	3.352 (9)		

Table 4

Hydrogen-bond geometry (Å, °) for (II).

<i>D</i> —H... <i>A</i>	<i>D</i> —H	H... <i>A</i>	<i>D</i> ... <i>A</i>	<i>D</i> —H... <i>A</i>
N1—H1...O4	0.86	2.20	2.908 (9)	140
N2—H2...O7	0.86	2.26	2.854 (9)	126
N5—H5...O8	0.86	2.20	2.914 (8)	141
N11—H11 <i>B</i> ...O4	0.86	2.12	2.973 (11)	172
N12—H12 <i>B</i> ...O2	0.86	2.13	2.962 (10)	163
N11—H11 <i>A</i> ...O8 ⁱⁱ	0.86	2.27	3.102 (10)	164
N12—H12 <i>A</i> ...O6 ⁱⁱⁱ	0.86	2.09	2.825 (9)	143

Symmetry codes: (ii) $-x + 1, -y, -z + 2$; (iii) $x + 1, y, z + 1$.

Two PF_6^- anions in (I) show orientational disorder. Around each P atom, there are two sets of possible positions, *viz.* F1*A*–F6*A* and F1*B*–F6*B* around P1, and F7*A*–F12*A* and F7*B*–F12*B* around P2. It was assumed that the disordered F atoms around each P atom would have the same isotropic displacement parameter. Furthermore, P–F distances were restrained to 1.55 (1) Å, and the 12 *cis* F...F distances within each PF_6^- anion were restrained to be equal. The sum of the occupation factors of sites *A* and *B* for each PF_6^- anion was restrained to unity. All H atoms of (I) were located in their idealized positions, with methyl C–H = 0.98 Å, aromatic C–H = 0.95 Å and guanidinate N–H = 0.88 Å, and included in the refinement using a riding model, with $U_{\text{iso}}(\text{H}) = 1.5U_{\text{eq}}(\text{methyl C}), 1.2U_{\text{eq}}(\text{aromatic C})$ and $1.2U_{\text{eq}}(\text{guanidinate N})$. In the final difference Fourier synthesis of (I), six residual peaks in the range 2.56–4.44 e Å⁻³ were observed, primarily near the Pt atoms.

For compound (II), the nitrate anion was observed to be disordered over two sites, *A* and *B*. The disordered atoms were assumed to have the same isotropic displacement parameter. Furthermore, the N–O distances were restrained to 1.22 (1) Å, the three O...O distances were restrained to be equal, and the nitrate anion was restrained to be planar. The two sites were assumed to be equally populated and therefore the occupation factors of the atoms were all fixed at 0.50. Two of the six water molecules were also observed to be disordered over two sites (O16*A*/O16*B* and O17*A*/O17*B*). For each of them, the disordered atoms were assumed to have the same isotropic displacement parameter, and the occupation factors of the atoms were fixed at 0.50, as for the nitrate geometry. All H atoms, except for those of the water molecules, were located in their idealized positions, with methyl C–H = 0.96 Å, aromatic C–H = 0.93 Å and guanidinate N–H = 0.86 Å, and included in the refinement using a riding model, with $U_{\text{iso}}(\text{H}) = 1.5U_{\text{eq}}(\text{methyl C}), 1.2U_{\text{eq}}(\text{aromatic C})$ and $1.2U_{\text{eq}}(\text{guanidinate N})$. In the final difference Fourier synthesis of (II), six residual peaks in the range 1.03–2.15 e Å⁻³ were observed near the Pt atoms.

For both compounds, data collection: *SMART* (Bruker, 2001); cell refinement: *SAINT* (Bruker, 2001); data reduction: *SAINT*; program(s) used to solve structure: *SHELXS97* (Sheldrick, 1997); program(s) used to refine structure: *SHELXL97* (Sheldrick, 1997); molecular graphics: *KENX* (Sakai, 2004); software used to prepare material for publication: *SHELXL97*, *TEXSAN* (Molecular Structure Corporation, 2001), *KENX* and *ORTEPII* (Johnson, 1976).

This work was partly supported by Grants-in-Aid for Scientific Research (B) (grant No. 14340223) and (A) (grant No. 17205008), and partly by a Grant-in-Aid for Scientific Research on Priority Areas (grant No. 16074216 of 434, ‘Chemistry of Coordination Space’), from the Ministry of Education, Culture, Sports, Science and Technology of Japan.

Supplementary data for this paper are available from the IUCr electronic archives (Reference: BM3021). Services for accessing these data are described at the back of the journal.

References

- Akiyama, N., Sato, N., Konno, Y., Sakai, K., Kajiwara, T. & Ito, T. (2000). Japan Symposium on Coordination Chemistry, Ritsumeikan University, 16–18 September, 2000. Paper No. 2P1-C08.
- Bruker (2001). *SAINT* (Version 6.22) and *SMART* (Version 5.625). Bruker AXS Inc., Madison, Wisconsin, USA.
- Johnson, C. K. (1976). *ORTEPII*. Report ORNL-5138. Oak Ridge National Laboratory, Tennessee, USA.
- Molecular Structure Corporation (2001). *TEXSAN*. Version 1.11r1. MSC, The Woodlands, Texas, USA.
- Sakai, K. (1996). Unpublished results.
- Sakai, K. (2004). *KENX*. Kyushu University, Japan.
- Sakai, K., Ishigami, E., Konno, Y., Kajiwara, T. & Ito, T. (2002). *J. Am. Chem. Soc.* **124**, 12088–12089.
- Sakai, K., Kurashima, M., Akiyama, N., Satoh, N., Kajiwara, T. & Ito, T. (2003). *Acta Cryst.* **C59**, m345–m349.
- Sakai, K., Takeshita, M., Tanaka, Y., Ue, T., Yanagisawa, M., Kosaka, M., Tsubomura, T., Ato, M. & Nakano, T. (1998). *J. Am. Chem. Soc.* **120**, 11353–11363.
- Sakai, K., Tanaka, Y., Tsuchiya, Y., Hirata, K., Tsubomura, T., Iijima, S. & Bhattacharjee, A. (1998). *J. Am. Chem. Soc.* **120**, 8366–8379.
- Schramm, C. J., Scaringe, R. P., Stojakovic, D. R., Hoffman, B. M., Ibers, J. A. & Marks, T. J. (1980). *J. Am. Chem. Soc.* **102**, 6702–6713.
- Sheldrick, G. M. (1996). *SADABS*. University of Göttingen, Germany.
- Sheldrick, G. M. (1997). *SHELXS97* and *SHELXL97*. University of Göttingen, Germany.
- Wimmer, S., Castan, C., Wimmer, F. L. & Johnson, N. P. (1988). *Inorg. Chim. Acta*, **142**, 13–15.
- Yokokawa, K. & Sakai, K. (2004). *Acta Cryst.* **C60**, m244–m247.